JOURNAL OF THEORETICAL
AND APPLIED MECHANICS
64, 2, pp. 145–163, Warsaw 2026
https://doi.org/10.15632/jtam-pl/221708

AN ADAPTIVE SEMI-EMPIRICAL FRAMEWORK FOR ROLLING RESISTANCE PREDICTION INCORPORATING TIRE MASS AND DYNAMIC GEOMETRIC PARAMETERS

Mohammad Sadegh NAEBI[1], Hamed RAEISIFARD[1*], Nader MOHAMMADI[2]

[1] *Department of Mechanical Engineering, WT.C., Islamic Azad University, Tehran, Iran*
[2] *Department of Mechanical Engineering, Pa.C., Islamic Azad University, Parand, Tehran, Iran*
*corresponding author, *ha.raeisifard@iau.ac.ir*

Rolling resistance (RR) is a key factor affecting vehicle energy efficiency and fuel consumption, and it is strongly influenced by tire design parameters. In this study, the effects of tire mass and key geometric parameters, including dynamic sidewall, dynamic diameter, and seated width, on RR are systematically investigated through experimental measurements and analytical modeling. Unlike conventional studies that primarily focus on applied load, this work emphasizes the influence of the tire's intrinsic mass and incorporates multiple design parameters within a unified framework. To better represent tire behavior under rolling conditions, dynamic (functional) geometric parameters are used instead of nominal values. Based on experimental data obtained under controlled conditions in accordance with ISO 28580, individual relationships between each parameter and RR are established using curve-fitting techniques. A comprehensive model is then developed by combining these effects through different weighting approaches. In particular, a novel sliding normalization model (MSN) is proposed to adaptively determine variable weighting coefficients. Unlike constant and sigmoid-based methods, the MSN approach adjusts parameter weights based on their normalized positions within the dataset range, thereby improving flexibility and predictive performance. The proposed model is validated using 27 tire samples, including 21 test tires and 6 additional tires not used in model calibration. The results show that the MSN approach achieves a lower prediction error than conventional weighting methods. The model demonstrates strong predictive capability within the investigated parameter ranges. It should be noted that the proposed framework is semi-empirical and is developed under controlled testing conditions, with operational variables such as inflation pressure, temperature, and velocity kept constant. Therefore, the model's applicability beyond the studied domain requires further investigation. Nevertheless, the present study provides a practical, adaptable approach for analyzing the influence of tire design parameters on RR and lays a foundation for future model development.

Keywords: tire rolling resistance (RR); parameters affecting RR; comprehensive model for RR; RR test.

1. Introduction

Rolling resistance (RR) is a critical factor influencing vehicle energy efficiency, fuel consumption, and environmental impact. As regulations on emissions and energy performance become increasingly stringent, improving tire performance has become a key focus in both academic research and industrial development. RR is primarily associated with energy dissipation mechanisms within the tire structure, including hysteresis losses in the rubber and tire deformation during rolling.

Previous studies have extensively investigated the effects of operational parameters, such as vertical load, inflation pressure, temperature, and speed, on RR. In particular, the effect of applied load (vehicle weight) has been widely analyzed and incorporated into both experimental and analytical models. However, comparatively less attention has been given to the role of the tire's intrinsic properties, especially the influence of the tire's own mass and its interaction with geometric design parameters. The investigation of RR has been approached through exper-

imental testing or finite element modeling (FEM). Experimental studies have provided direct measurements of rolling forces under varying loads, velocities, and material conditions. However, such methods are time-intensive and costly, as they require specialized testing drums and the fabrication of tire samples.

A fundamental understanding of RR is closely related to energy dissipation mechanisms within the tire structure. Walter and Conant (1974) demonstrated that RR primarily originates from hysteresis losses in the viscoelastic materials of the tire. During rolling, cyclic deformation of the tire leads to continuous energy dissipation, as part of the mechanical energy is converted into heat and cannot be fully recovered. Their work revealed that these energy losses depend not only on material properties but also on tire structural characteristics and the nature of deformation. This indicates that RR is inherently governed by both material behavior and tire design parameters.

Further studies have emphasized the role of tire design and material composition in RR. Martini (1983) demonstrated that tread compounding significantly affects energy losses, as modifications in rubber formulation can alter hysteresis behavior. However, improvements in RR are often accompanied by trade-offs with other performance characteristics, such as traction and wear resistance. This indicates that tire performance optimization is inherently a multi-parameter problem involving both material and structural design considerations.

In addition to material effects, the influence of design and construction parameters has been widely investigated. Walter (1983) analyzed the impact of several key design variables on RR and cornering force, showing that tire performance is strongly affected by the combined influence of multiple parameters. The study also demonstrates that improvements in one performance aspect may affect others, underscoring the multi-parameter, interdependent nature of tire design.

Recent studies have highlighted the importance of testing conditions in RR measurements. Ejsmont *et al.* (2025) investigated the influence of temperature on RR measurements and demonstrated that tire behavior is highly sensitive to thermal conditions. Due to viscoelastic effects, increasing temperature reduces material stiffness and hysteresis losses, thereby lowering RR. The study showed that RR values vary significantly during the heating phase and emphasized that accurate measurements must be performed under thermal equilibrium conditions. These findings highlight the critical role of temperature control and thermal history in obtaining reliable RR data. In addition, Ejsmont *et al.* (2024) compared different RR measurement methods and surface conditions, demonstrating that measured values vary significantly depending on testing approach and contact characteristics. The study showed that factors such as surface roughness and testing configuration influence tire deformation and energy dissipation, leading to discrepancies between laboratory and real-world results. These findings indicate that RR is not an intrinsic constant, but rather a system-dependent parameter influenced by measurement conditions and surface interactions.

More recent studies have adopted combined experimental and numerical approaches to analyze tire performance. Liang *et al.* (2020) evaluated RR and grip characteristics using both testing and simulation, and demonstrated that improvements in RR are often associated with reductions in grip performance. Their findings highlight the multi-objective nature of tire design, where performance optimization requires balancing competing criteria. Comprehensive reviews have further emphasized the multi-factor nature of RR.

Ydrefors *et al.* (2021) provided a comprehensive review demonstrating that RR is governed by complex interactions among material properties, tire design, and operating conditions. While hysteresis losses in viscoelastic materials are the primary source of energy dissipation, the study showed that factors such as temperature, load, inflation pressure, and speed significantly influence tire deformation behavior and energy losses. Their findings reveal that RR is inherently a multifactor, nonlinear phenomenon and cannot be accurately described by a single parameter.

Xu *et al.* (2025) demonstrated that advanced material engineering at the rubber-filler interface can significantly improve tire performance. By introducing chain difunctionalization

in styrene-butadiene rubber via thiol-ene click reactions, the interfacial interaction with silica was substantially enhanced, leading to improved filler dispersion and a more stable rubber-filler network. This resulted in reduced hysteresis losses and a significant decrease in RR, while simultaneously improving wet grip and wear resistance. These results show that RR is not only governed by macroscopic design parameters but is also strongly influenced by molecular-level interfacial phenomena.

Pillai and Fielding–Russell (1992) introduced an energy-based framework for evaluating RR by defining a whole-tire hysteresis ratio. They developed a simple equation for tire RR, in terms of the whole-tire hysteresis ratio, tire load, and footprint dimensions based on energetic considerations. Their approach established a direct relationship between RR and the energy dissipated during cyclic deformation, providing a macroscopic metric that links viscoelastic material behavior to overall tire performance. This work demonstrated that RR can be fundamentally interpreted as a manifestation of energy loss within the tire structure.

On the other hand, numerical studies using FEM and thermo-mechanical simulations have enabled predictive analysis of RR based on viscoelastic properties. However, they often depend on empirical assumptions and may overlook parameter interdependencies.

Ebbott *et al.* (1999) investigated the coupled thermo-mechanical behavior of tires using finite element analysis and demonstrated that RR is strongly influenced by temperature evolution within the tire. Cyclic deformation generates heat, which alters viscoelastic properties and hysteresis losses, creating a nonlinear feedback mechanism. Their results indicate that accurate prediction of RR requires simultaneous consideration of thermal and mechanical effects.

Shida *et al.* (1999) demonstrated that RR can be effectively estimated using static finite element analysis by incorporating equivalent hysteresis effects. Their approach significantly reduced computational complexity while maintaining reasonable accuracy, thus highlighting the practicality of numerical modeling in tire performance prediction. However, the use of simplified static representations also indicates limitations in fully capturing coupled dynamic and rate-dependent behaviors.

Luchini *et al.* (2001) studied tire RR for a group of radial medium truck tires, both experimentally and numerically (FEA modeling). They investigated the effect of tread depth on tire RR and demonstrated that increasing tread depth increases energy dissipation through greater cyclic deformation of the rubber. Their results showed a clear positive correlation between tread depth and RR, indicating that even small geometric variations can significantly influence hysteresis losses. This study highlights the strong dependence of RR on geometric design parameters and the trade-off between energy efficiency and traction performance.

Ma *et al.* (2007) developed an energy-based model to compute RR by analyzing hysteresis losses in viscoelastic rubber materials. Their approach demonstrated that RR arises from cyclic energy dissipation during deformation and can be quantitatively predicted from material properties. The study provided a fundamental link between viscoelastic behavior and tire performance, emphasizing that RR is primarily governed by material-induced energy losses.

Wang *et al.* (2018) proposed a region-based framework for RR analysis, demonstrating that energy dissipation is spatially non-uniform within tire structures. By dividing the tire into crown and non-crown regions and performing finite element-based sensitivity analysis, they showed that the crown region, particularly the tread, dominates RR with nearly 70 % contribution. At the same time, other components such as the sidewall, carcass, and apex contribute to the remaining portion. The study further revealed that different structural parameters exhibit location-dependent sensitivity, indicating that RR is governed by both the magnitude and spatial distribution of energy loss. This work highlights the limitations of purely global models and underscores the importance of localized structural optimization.

Mangal *et al.* (2021) introduced a variable modulus framework to optimize RR by tailoring the spatial distribution of mechanical properties within the tire. Their results showed that RR is closely linked to viscoelastic deformation, where an increased modulus reduces hysteresis losses,

while a lower modulus enhances grip. By strategically varying the modulus across different regions, the study demonstrated the potential to mitigate the traditional trade-off between RR and traction. This work highlights the critical role of material distribution in governing tire energy dissipation and performance.

Jittham *et al.* (2022) employed finite element analysis to investigate the RR behavior of pneumatic and solid tires, providing insight into the role of structural configuration and material behavior. Their results showed that tire structure significantly affects deformation patterns, stress distribution, and energy dissipation mechanisms. These findings demonstrate that RR is not solely determined by material properties but is strongly influenced by the interactions among structure, material behavior, and contact mechanics. They showed that increasing the contact area reduced tire RR, whereas increasing the tread depth increased it.

Ydrefors *et al.* (2024) investigated RR at low temperatures and found that lower temperatures significantly alter the viscoelastic behavior of tire materials. Increased stiffness and changes in hysteresis characteristics lead to higher energy dissipation and, consequently, increased RR. The study further demonstrated that tire behavior under low-temperature conditions deviates from standard testing assumptions, underscoring the need to account for real-world operating conditions in RR analysis.

Most existing studies examine individual parameters independently, whereas in practical tire design, multiple parameters, such as diameter, sidewall, and seated width, are simultaneously varied. This limitation restricts the applicability of existing models when multiple design variables are modified concurrently. Furthermore, conventional approaches often rely on nominal geometric parameters that may not accurately reflect tire behavior under rolling conditions, where deformation alters the effective geometry.

While previous research has extensively examined the influence of applied load on RR, the tire's own mass has not been explicitly treated as a separate parameter. This may be attributed to the dominant influence of external loading conditions in typical operating scenarios, as well as the practical difficulty of isolating tire mass effects experimentally. In this study, an effort is made to account for tire mass within the modeling framework explicitly.

To address these limitations, the present study investigates the combined effects of key tire design parameters, including tire mass, dynamic sidewall, dynamic diameter, and seated width, on RR. In contrast to nominal values, dynamic (functional) geometric parameters better capture the tire's actual deformation characteristics during rolling.

Based on experimental measurements conducted under controlled conditions in accordance with ISO 28580, individual relationships between each parameter and RR are established using curve-fitting techniques. A comprehensive analytical model is then developed by combining these effects within a unified framework. The originality of this work lies in the formulation of an analytical structure that integrates the independent empirical relations of each design factor into a unified model.

Unlike conventional weighting approaches such as constant or sigmoid-based models, which rely on predefined functional forms, the present study introduces a sliding normalization model (MSN) to determine weighting coefficients in a data-adaptive manner. In this approach, the contribution of each parameter is dynamically adjusted based on its relative position within the dataset range, allowing the model to better reflect variations in parameter influence without imposing prior assumptions. Therefore, the MSN provides a more general and adaptable framework for modeling RR than the other two approaches.

It should be noted that the proposed framework is semi-empirical, in which the total RR is represented as a weighted superposition of individual parameter effects. Although explicit interaction terms are not included, variable weighting coefficients enable indirect consideration of concurrent parameter influences. The proposed model is validated using independent experimental data and demonstrates improved predictive performance compared to conventional weighting approaches. However, the model is developed within a specific parameter range and

under controlled testing conditions, and its applicability beyond this domain requires further investigation.

The remainder of this paper is organized as follows. Section 2 describes the experimental work and data acquisition. Section 3 presents the analytical modeling. Section 4 presents a comprehensive analytical model, and finally, Section 5 discusses the results and model validation.

2. Experimental work

An ISO 28580-based RR testing machine (as shown in Fig. 1) is employed to measure the RR of the test tires. The system includes controlled loading, speed, and environmental conditions to ensure repeatability and accuracy of the measurements.

Fig. 1. Schematic of the experimental setup used for RR measurements in accordance with ISO 28580.

Prior to experimentation, the Design of Experiments (DoE) framework was established, comprising the selected parameters, the number of tests, replications, environmental conditions, permissible and impermissible errors, estimates and approximations, testing procedures, standards, requirements, and constraints. All aspects of the test – requirements, conditions, specifications, tolerances, errors, correction factors, and the testing procedure – conformed to ISO 28580 (2018 edition) and ECE Regulation No. 117 (2016 edition).

The RR measurements were conducted using a drum-type testing machine. The apparatus consists of a steel drum with a 2 m diameter, designed to minimize vibration and ensure stable test conditions. During the tests, the tire was mounted on the spindle and brought into contact with the rotating drum, where a normal load equivalent to 80 % of the tire's maximum allowable load was applied. All tests were performed under controlled laboratory conditions, with an ambient temperature maintained at 25 °C, a constant inflation pressure of 210 kPa ($\pm$3 kPa), and a steady rolling speed of 22.2 m/s ($\pm$0.14 m/s). Prior to data acquisition, each tire underwent a warm-up phase of approximately 30 minutes to reach thermal equilibrium. The RR force was then measured under steady-state conditions, and multiple measurements were performed to ensure repeatability and reliability of the results. All test procedures, tolerances, correction factors, and measurement protocols were implemented in accordance with ISO 28580 requirements to ensure consistency and comparability of the obtained data. Operational parameters such as inflation pressure, temperature, and speed were kept constant in order to isolate the effects of tire design parameters. Incorporating these operational variables into the model is considered a direction for future research.

Table 1 shows selected parameters related to the testing equipment and testing conditions.

2.1. Design parameters and test tires

This study focuses on the design-parameter group among the four parameter groups – tire design parameters, environmental parameters, tire performance parameters, and road parame-

Table 1. Parameters related to the testing equipment and testing conditions.

Parameter	Value
Drum diameter of the RR machine	2 m
Ambient temperature in the drum, 1 meter above the drum, and 15 centimeters below the drum	25 °C
Linear test velocity / Speed of the drum (Class C1 tires)	22.2 m/s (±0.14 m/s)
Tire acceleration	0.14 m/s^2
Tire pressure (ambient air)	210 kPa (±3 kPa)
Tire warm-up time	30 min
Tire Spindle force (Class C1 tires)	Min: 100 N
	Max: 200 N
The load applied to the tire is 80% of the tire's maximum allowable load	

ters – that influence RR. Unlike the other three groups, design parameters are specific to the tire manufacturer and designer. The study meticulously and comprehensively analyzes four parameters from the design-parameter group: tire mass, overall diameter, sidewall, and seated width. To do this, four sets of test tires are selected, each with only one of these design parameters fixed, while the remaining parameters vary.

In the existing literature, RR has been predominantly analyzed in relation to external load, which represents the operational weight applied to the tire. Consequently, the contribution of the tire's own mass has not been explicitly isolated or systematically investigated. This is likely due to the experimental challenges associated with decoupling tire mass from other design parameters. The present work addresses this limitation by explicitly considering tire mass as an independent variable. By incorporating tire mass as an independent parameter, the proposed model provides a more comprehensive representation of RR behavior. It is foreseeable that an increase in tire weight will lead to greater heat generation, increased energy loss, and consequently higher RR. To quantify tire mass effects, two test tire series were selected. Each series is geometrically identical to the others, but their compounds – and hence their masses – differ (as shown in Table 2). The compounds employed in this study are of three types, and the densities of these compounds fall between 0.9 g/cm^3 and 1.2 g/cm^3.

Herein, the examination of the influence of the tire sidewall on RR presents a fundamental difference from prior research. The numerical value of the tire sidewall is computed from the tire diameter rather than from the tire width. In addition, the dynamic sidewall derived from the dynamic diameter is employed here. Because the aspect ratio (the sidewall-to-width ratio) is a bivariate parameter, and its consideration does not permit precise isolation of the individual effects of tire sidewall and tire width on RR, the effect of tire sidewall, instead of the aspect ratio, is examined here. In evaluating the influence of tire sidewall on RR, not only must all geometric parameters (except for the sidewall) of the tested tires be identical, but the material of the sidewall of the tires must also be the same. In this study, five test tires are used, each with a different sidewall (and mass), while keeping other design parameters, including width, constant (as shown in Table 2).

The nominal radius, or the unloaded radius of a tire, also referred to as the overall radius, is one of the important parameters that affect tire RR. The static radius for a stationary vehicle, depending on the sidewall value and the tire compound, typically has about 5 % to 10 % sag relative to the nominal radius. In contrast, the dynamic radius, which depends on vehicle and wind velocities and the tire's overall stiffness, is larger than the static radius. Here, the tire's dynamic radius is examined. To evaluate tire diameter, the tire pressure and load applied to all test tires must match the standard values; otherwise, these influential parameters may introduce errors in the evaluation of the tire diameter's effect on RR. In this study, five test tires are

Table 2. RR values measured for the test tires.

Design parameters	Tire size	Dynamic sidewall [m]	Dynamic diameter [m]	Seated width [m]	Mass [kg]	RR_0 [N/kN]	RR_C
Mass	205/50R17	0.092	0.566	0.164	9.07	9.15	9.15
		0.093	0.574		9.34	9.43	9.43
		0.095	0.581		9.62	9.65	9.65
	215/55R18	0.106	0.660	0.174	11.135	8.84	8.84
		0.1085	0.670		11.350	9.08	9.08
		0.11	0.677		11.530	9.21	9.21
Sidewall	225/55R19	0.1107	0.704	0.174	12.640	9.45	9.45
	225/60R18	0.1224	0.702		12.810	9.52	9.367
	225/65R17	0.1331	0.698		13.050	9.60	9.231
	225/70R16	0.1453	0.697		12.550	9.10	9.18
	225/75R15	0.1565	0.694		12.300	8.81	9.15
Diameter	205/60R13	0.113	0.556	0.164	7.640	8.9	9.80
	205/60R14	0.112	0.580		8.155	9.14	9.644
	205/60R15	0.112	0.605		8.715	9.31	9.31
	205/60R16	0.111	0.627		9.270	9.20	8.645
	205/60R17	0.112	0.655		9.810	9.50	8.515
Seated width	205/55R16	0.1013	0.609	0.164	8.350	9.22	9.22
				0.172		8.85	8.85
				0.1756		8.40	8.40
				0.1795		8.22	8.22
				0.1808		8.17	8.17

employed, differing only in diameter and mass, and all other design parameters and practical conditions (tire pressure, applied load, tire velocity, etc.) are kept constant (as shown in Table 2).

The seated width of a tire, a design parameter with a fixed value, is defined as the width of the tire's ground-contact patch under a standard load and inflation pressure. Herein, variations in seated width due to changes in the tire pressure, vehicle weight, or the load applied to the tire are not considered. An increase in seated width leads to an enlargement of the tire-ground contact area, a reduction in vertical pressure, less localized deformation, lower energy losses, and, consequently, a reduction in tire RR. In this study, five test tires are employed, differing only in seated width, while all other design parameters remain the same (as shown in Table 2).

2.2. Test results

The results of the RR tests (RR_0) for four design parameters – mass, sidewall, diameter, and seated width – are presented in Table 2.

3. Analytical model

3.1. Mass effect on RR

Using the Curve Fitting Toolbox-MATLAB, a linear regression equation for the RR values as a function of the tire mass is approximated as follows:

$$\begin{aligned} \mathrm{RR}(M_1) &= 0.9083\, M_1 + 0.9232, \\ \mathrm{RR}(M_2) &= 0.9425\, M_2 - 1.6427, \end{aligned} \tag{3.1}$$

where RR is the RR value (RR_0 values are shown in Table 2) and M is the mass of the test tires. The subscripts 1 and 2 denote the two test tire series used for evaluating the effect of the tire mass parameter on RR.

Equation (3.1) shows that the change in tire RR with mass is linear, with a slope of 90 %. Although the tires used to examine the effect of mass are geometrically identical, and generalizing to the entire range of tires is challenging, examining tires from the Michelin and Bridgestone brands (tires are geometrically identical but with different densities) also suggests that a linear regression equation with a slope close to 100 % for RR as a function of the tire mass can be approximated. By extending this equation to all tires in the 8 to 12 [kg] range (which includes most passenger tires), a linear regression equation for the influence of mass on RR is approximated as follows (it is shown in Fig. 2):

$$\mathrm{RR}(M) = 0.9\,M + 0.987. \tag{3.2}$$

The predicted RR values from the fitted mass-effect curve are presented in Table 3.

Table 3. Predicted RR values from the fitted curve (mass effect).

Tire size	Mass [kg]	RR_0	RR_C	RR_1
205/50R17	9.07	9.15	9.15	9.15
	9.34	9.43	9.43	9.393
	9.62	9.65	9.65	9.645
215/55R18	11.135	8.84	8.84	11.009
	11.350	9.08	9.08	11.202
	11.530	9.21	9.21	11.364

The derived linear relationship between tire mass and RR is valid over the investigated mass range (8 kg to 12 kg), which corresponds to typical passenger-car tires. Application of this relationship outside this range may introduce additional uncertainty. It should be noted that the proposed mass-RR relationship is derived empirically based on experimental data within the investigated mass range and should not be extrapolated beyond this domain. The non-zero intercept of the fitted function arises from the curve-fitting process. It does not represent a physically meaningful condition, since a tire of zero mass is not physically realizable.

As shown in Fig. 2, RR increases approximately linearly with tire mass for geometrically identical tires. This trend can be attributed to the increased material volume and internal hysteresis losses associated with heavier tires. The observed linear behavior over the investigated mass range (8 kg to 12 kg) supports the use of a first-order approximation to model the mass–RR

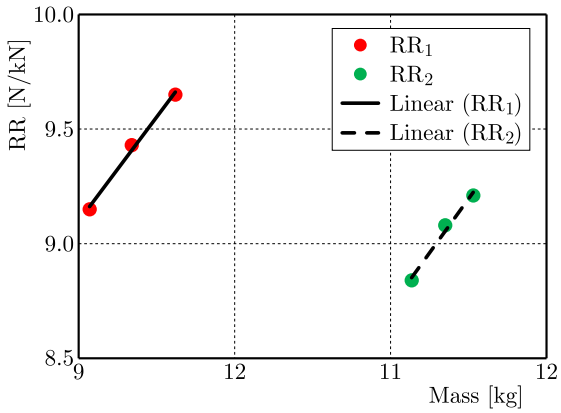

Fig. 2. Relationship between tire mass and RR for tires with identical geometric characteristics. The results indicate an approximately linear trend within the investigated mass range, supporting the use of a first-order approximation.

relationship. It should be noted, however, that this linearity is valid within the studied domain and may not necessarily extend beyond this range.

3.2. Sidewall effect on RR

In examining the effect of tire sidewall and diameter parameters on RR, the test specimens not only have different sidewall and diameter values but also vary in mass (as shown in Table 2). This difference in the mass of the test specimens is due, from a technical standpoint, to the fact that it is not feasible to produce tires with different sidewall and diameter values that have the same mass. Therefore, by equalizing tire mass, the influence of mass changes on RR must be removed from the test results to ensure that the findings reflect solely the effects of tire sidewall or diameter parameters on RR. Using Eq. (3.2), the influence of mass changes on the RR values is removed (see RR_C in Table 2).

Using the Curve Fitting Toolbox-MATLAB, the quadratic and cubic equations are identified as the best candidates for the fitting curve of the RR values as a function of the sidewall. First, the accuracy of these two models is assessed using the root-mean-square (RMS) percentage error (% RMSE) criterion:

$$\mathrm{RMSE}\,(\%) = 100\frac{\sqrt{\dfrac{\sum\limits_{i=1}^{N}\left[\mathrm{RR}_C(i)-\mathrm{RR}_{\mathrm{Model}}(i)\right]^2}{N}}}{\sum\limits_{i=1}^{N}\dfrac{\mathrm{RR}_C(i)}{N}}, \tag{3.3}$$

where RR_C are the corrected test results for RR (RR_C can be seen in Table 2), and $\mathrm{RR}_{\mathrm{Model}}$ are the predicted RR values from the fitted curve (RR_2 and RR_3 can be seen in Table 4). Additionally, N is the number of data points.

Table 4. Predicted RR values from the fitted curve (sidewall effect).

Tire size	RR_C	RR_2	RR_3
225/55R19	9.45	9.46	9.453
225/60R18	9.367	9.338	9.352
225/65R17	9.231	9.251	9.251
225/70R16	9.18	9.182	9.166
225/75R15	9.15	9.146	9.153

From Table 4 and using Eq. (3.3), the RMSE values are computed for each model, therefore

$$\mathrm{RMSE}_2 = 0.18\,\%, \qquad \mathrm{RMSE}_3 = 0.14\,\%.$$

Considering the RSME values, both models are acceptable. Here, the more straightforward quadratic equation is used. It should be noted that although higher-order polynomial models (e.g., cubic) were also evaluated, they did not provide a significant improvement in accuracy compared to quadratic models. Therefore, quadratic functions were selected to maintain model simplicity and avoid potential overfitting. The fitted curve for the RR values as a function of the tire sidewall (S) is expressed as follows (it is shown in Fig. 3):

$$\mathrm{RR}(S) = 105.22\,S^2 - 34.986\,S + 12.044. \tag{3.4}$$

Figure 3 illustrates the effect of the dynamic sidewall on RR after applying mass correction (RR_C). The results indicate a clear dependency of RR on sidewall height. This behavior can be explained by the role of sidewall deformation in energy dissipation mechanisms. Tires with larger sidewall values tend to exhibit different deformation patterns, which directly influence hysteresis losses and, consequently, RR.

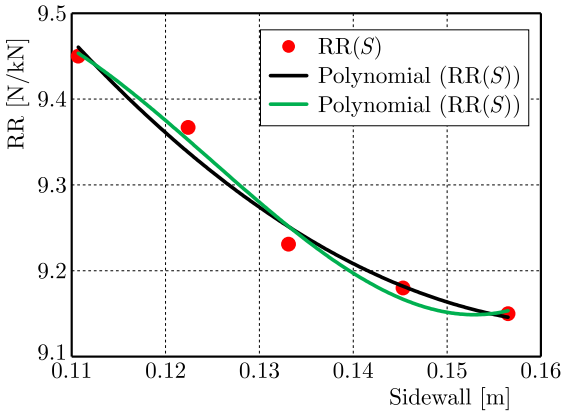

Fig. 3. Effect of dynamic sidewall on corrected rolling resistance (RR_C). Experimental data after removing the influence of tire mass are presented as red markers, while quadratic and cubic regression fits are shown by black and green lines, respectively.

3.3. Diameter effect on RR

The quadratic and cubic equations are identified as the best candidates for fitting the RR values as a function of diameter. From the predicted RR values from the fitted curve (RR_2 and RR_3 can be seen in Table 5) and using Eq. (3.3), the RMSE values are computed for each model, thus

$$\mathrm{RMSE}_2 = 1.5\,\%, \qquad \mathrm{RMSE}_3 = 1\,\%.$$

Table 5. Predicted RR values from the fitted curve (diameter effect).

Tire size	RR_C	RR_2	RR_3
205/60R13	9.80	9.809	9.730
205/60R14	9.644	9.514	9.654
205/60R15	9.310	9.191	9.240
205/60R16	8.645	8.893	8.812
205/60R17	8.515	8.495	8.494

Considering the RSME values, both models are acceptable. Here, the more straightforward quadratic equation is used. Therefore, the fitted curve for the RR values as a function of the diameter (D) is expressed as follows (it is shown in Fig. 4):

$$\mathrm{RR}(D) = -13.269\,D^2 + 2.8\,D + 12.354. \tag{3.5}$$

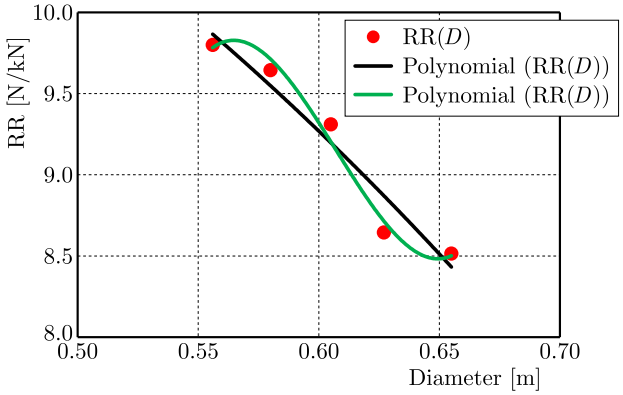

Fig. 4. Effect of dynamic diameter on RR_C. Experimental data, after removing the influence of tire mass, are presented as red markers, and quadratic and cubic regression fits are shown by black and green lines, respectively.

As shown in Fig. 4, increasing the dynamic diameter generally reduces RR. This can be physically interpreted as larger diameters reducing the curvature of the contact region, thereby decreasing cyclic deformation and associated energy losses per revolution. The trend is consistent across the dataset under investigation and supports including diameter as a key design parameter.

3.4. Seated width effect on RR

The quadratic and cubic equations are identified as the best candidates for fitting the RR values as a function of seated width. From the predicted RR values from the fitted curve (RR_2 and RR_3 can be seen in Table 6) and using Eq. (3.3), the RMSE values are computed for each model, hence

$$\mathrm{RMSE}_2 = 0.068\,(0.8\,\%), \qquad \mathrm{RMSE}_3 = 0.107\,(1.25\,\%).$$

Table 6. Predicted RR values from the fitted curve (seated width effect).

Tire size	Seated width [m]	RR_0	RR_2	RR_3
205/55R16	0.164	9.22	9.236	9.321
	0.172	8.85	8.753	8.941
	0.1756	8.40	8.511	8.532
	0.1795	8.22	8.230	8.287
	0.1808	8.17	8.132	8.299

Considering the RSME values, both models are acceptable. Here, the more straightforward quadratic equation is used. Therefore, the fitted curve for the RR values as a function of the seated width (W) is expressed as follows (it is shown in Fig. 5):

$$\mathrm{RR}(W) = -608.9\,W^2 + 144.21\,W + 1.9629. \tag{3.6}$$

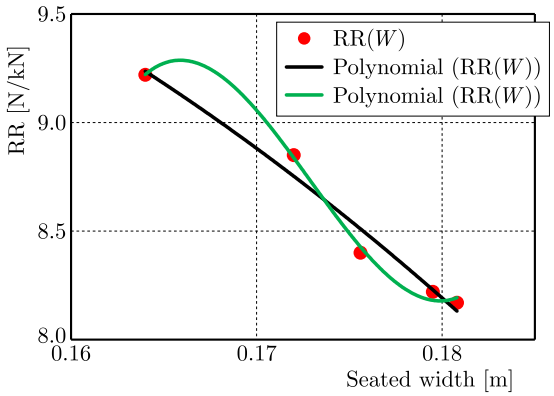

Fig. 5. Effect of seated width on rolling resistance (RR_0). Experimental data are presented as red markers, and quadratic and cubic regression fits are shown by black and green lines, respectively.

Figure 5 presents the influence of seated width on RR. The results suggest that variations in seated width affect the contact patch geometry and stress distribution, which in turn influence deformation behavior and hysteresis losses. Although the relationship is not strictly linear, the observed trend confirms that seated width is an important parameter in RR modeling.

4. Comprehensive analytical model

In tire design, it is essential to have a comprehensive model that can simultaneously predict the effects of tire geometric parameters (sidewall, diameter, and seated width) and mass on RR. This comprehensive model can be expressed in the form of Eq. (4.1):

$$\mathrm{RR}(S, D, W, M) = C(S)\mathrm{RR}(S) + C(D)\mathrm{RR}(D) + C(W)\mathrm{RR}(W) + C(M)\mathrm{RR}(M), \tag{4.1}$$

in which the function $\mathrm{RR}(S, D, W, M)$ is the comprehensive model for RR, and the coefficients $C(X)$ represent the contribution and weight of parameter X in the comprehensive model of RR. Herein, three approaches to determining $C(X)$ coefficients are presented: one assumes the coefficients are constant, and two assume the coefficients are variable.

It should be noted that the proposed formulation is semi-empirical, in which the total RR is represented as a weighted superposition of individual parameter effects. Although explicit interaction terms are not included, the use of variable weighting coefficients in the MSN framework permits indirect consideration of concurrent parameter influences.

4.1. Comprehensive model with constant coefficients

The constant coefficient approach is presented primarily as a baseline model for comparison. As expected, its predictive performance is lower than that of the adaptive weighting approaches. To determine the constant coefficients C, mid tires are selected from each set of test tires (as shown in Table 7), and the geometric parameters of the selected tires – including sidewall, diameter, and seated width – as well as their masses and the predicted RR values from the fitted curves (RR_1 and RR_2) are substituted into the comprehensive model.

Table 7. Mid tire specifications.

Design parameters	Tire size	Dynamic sidewall	Dynamic diameter	Seated width	Mass
Mass	205/50R17	0.093	0.574	0.164	9.34
Sidewall	225/65R17	0.1331	0.698	0.174	12.640
Diameter	205/60R15	0.112	0.605	0.164	8.715
Seated width	205/55R16	0.1013	0.609	0.1756	8.350

Therefore, the equations of the comprehensive model can be simplified as follows:

$$\begin{aligned}
9.251\,C_1 + 7.844\,C_2 + 8.620\,C_3 + 12.363\,C_4 &= 9.251,\\
9.445\,C_1 + 9.191\,C_2 + 9.236\,C_3 + 8.831\,C_4 &= 9.191,\\
9.580\,C_1 + 9.138\,C_2 + 8.511\,C_3 + 8.502\,C_4 &= 8.511,\\
9.70\,C_1 + 9.098\,C_2 + 9.236\,C_3 + 9.393\,C_4 &= 9.393.
\end{aligned}$$

From solving the above system of equations, the coefficients C_i are obtained. Then the coefficients are normalized to lie in the range $[-1, 1]$ and finally substituted into Eq. (4.1), yielding a comprehensive model with constant coefficients. Therefore

$$\begin{aligned}
\mathrm{RR}(S, D, W, M) = {} & 0.244(105.220\,S^2 - 34.986\,S + 12.044)\\
& + 0.288(-13.269\,D^2 + 2.80\,D + 12.354)\\
& + 0.458(-608.90\,W^2 + 144.21\,W + 1.9629)\\
& + 0.01(0.9\,M + 0.987).
\end{aligned} \tag{4.2}$$

4.2. Comprehensive model with sigmoid variable coefficients

An analysis of plots derived from the analytical equations of the geometric parameters and mass reveals an S-shaped, or sigmoid, behavior. Accordingly, the sigmoid function is adopted to determine the coefficients of the comprehensive model. The sigmoid model employed is expressed as follows:

$$\frac{\mathrm{RR}(X)_{\max} - C(X)}{C(X) - \mathrm{RR}(X)_{\min}} = \exp[K_X(X - X_C)]. \tag{4.3}$$

The sigmoid variable coefficients are therefore determined as:

$$C(X) = \mathrm{RR}(X)_{\min} + \frac{\mathrm{RR}(X)_{\max} - \mathrm{RR}(X)_{\min}}{1 + \exp[K_X(X - X_C)]}, \tag{4.4}$$

where $\mathrm{RR}(X)_{\max}$ and $\mathrm{RR}(X)_{\min}$ represent the maximum and minimum values of RR predicted from the fitted curve corresponding to parameter X, K_X denotes the slope coefficient of the sigmoid function, and X_C denotes the value of parameter X at which RR is at its average value (it can be seen in Table 8 to Table 11). To determine coefficient K_X, the data corresponding to each parameter (as shown in Table 8 to Table 11) are substituted into the sigmoid model (Eq. (4.4)), the corresponding K_X values are computed, and the most accurate K_X coefficient is selected using the RMS criterion.

Table 8. Data corresponding to mass parameter.

M	RR	$\mathrm{RR}(X)_{\max}$	$\mathrm{RR}(X)_{\min}$	$\mathrm{RR}(X)_{\mathrm{avg}}$	X_C	K_X
9.07	9.15	9.645	9.15	9.398	9.345	−0.84
9.34	9.393					
9.62	9.645					

Table 9. Data corresponding to sidewall parameter.

S	RR	$\mathrm{RR}(X)_{\max}$	$\mathrm{RR}(X)_{\min}$	$\mathrm{RR}(X)_{\mathrm{avg}}$	X_C	K_X
0.1107	9.460	9.460	9.146	9.276	0.1297	110
0.1224	9.338					
0.1331	9.251					
0.1453	9.182					
0.1565	9.146					

Table 10. Data corresponding to diameter parameter.

D	RR	$\mathrm{RR}(X)_{\max}$	$\mathrm{RR}(X)_{\min}$	$\mathrm{RR}(X)_{\mathrm{avg}}$	X_C	K_X
0.556	9.809	9.809	8.495	9.152	0.608	45
0.580	9.514					
0.605	9.191					
0.627	8.893					
0.655	8.495					

Table 11. Data corresponding to seated width parameter.

W	RR	$\mathrm{RR}(X)_{\max}$	$\mathrm{RR}(X)_{\min}$	$\mathrm{RR}(X)_{\mathrm{avg}}$	X_C	K_X
0.164	9.236	9.236	8.132	8.684	0.1731	350
0.172	8.753					
0.1756	8.511					
0.1795	8.230					
0.1808	8.132					

Therefore, the sigmoid variable coefficients are expressed as:

$$\begin{aligned} C(M) &= 9.150 + \frac{0.495}{1+\exp\left[-0.84(M-9.345)\right]}, \\ C(S) &= 9.146 + \frac{0.314}{1+\exp\left[110(S-0.1297)\right]}, \\ C(D) &= 8.495 + \frac{1.314}{1+\exp\left[45(D-0.608)\right]}, \\ C(W) &= 8.132 + \frac{1.104}{1+\exp\left[350(W-0.1731)\right]}. \end{aligned} \tag{4.5}$$

The coefficients are then normalized and finally substituted into Eq. (4.1), yielding a comprehensive model with sigmoidal variable coefficients.

4.3. MSN comprehensive model

Here, a new model (research innovation) named the "Slide Model" (MSN) is presented. As shown in Fig. 6, the MSN model is expressed as follows:

$$\frac{\ln Y_{\max} - \ln Y(X)}{\ln Y_{\max} - \ln Y_{\min}} = \left(\frac{X - X_{\min}}{X_{\max} - X_{\min}}\right)^2. \tag{4.6}$$

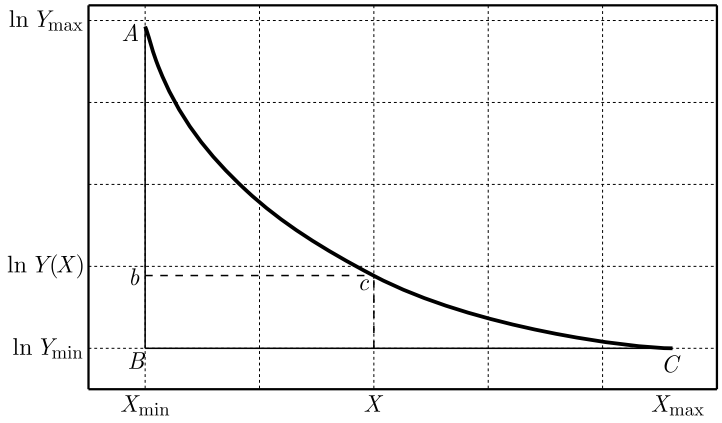

Fig. 6. MSN model used to determine the coefficients of the comprehensive model.

The quantity $Y(X)/Y_{\max}$ is regarded as the variable coefficient $C(X)$, and Eq. (4.6) is then rewritten as follows:

$$\begin{aligned} \ln C(X) &= \ln\left(\frac{\mathrm{RR}(X)_{\min}}{\mathrm{RR}(X)_{\max}}\right)\left(\frac{X - X_{\min}}{X_{\max} - X_{\min}}\right)^2, \\ C(X) &= \exp\left[\left(\frac{\mathrm{RR}(X)_{\min}}{\mathrm{RR}(X)_{\max}}\right)\left(\frac{X - X_{\min}}{X_{\max} - X_{\min}}\right)^2\right]. \end{aligned} \tag{4.7}$$

The above equation for the mass parameter is rewritten as follows:

$$C(X) = \exp\left[\left(\frac{\mathrm{RR}(X)_{\min}}{\mathrm{RR}(X)_{\max}}\right)\left(\frac{X - X_{\max}}{X_{\max} - X_{\min}}\right)^2\right]. \tag{4.8}$$

All parameters of the two relations above were listed in Table 8 to Table 11. Therefore, the MSN variable coefficients are expressed as:

$$\begin{aligned} C(M) &= \exp\left[\left(\frac{9.15}{9.645}\right)\left(\frac{M - 9.62}{0.55}\right)^2\right], \\ C(S) &= \exp\left[\left(\frac{9.146}{9.460}\right)\left(\frac{S - 0.1107}{0.0458}\right)^2\right], \\ C(D) &= \exp\left[\left(\frac{8.495}{9.809}\right)\left(\frac{D - 0.556}{0.099}\right)^2\right], \\ C(W) &= \exp\left[\left(\frac{8.132}{9.236}\right)\left(\frac{W - 0.164}{0.0168}\right)^2\right]. \end{aligned} \tag{4.9}$$

The coefficients are then normalized and finally substituted into Eq. (4.1), yielding a comprehensive model with MSN variable coefficients.

It should be noted that the proposed formulation in Eq. (4.1) is semi-empirical in nature, where the total RR is represented as a weighted superposition of individual parameter effects. Although explicit interaction terms are not included, the use of variable weighting coefficients in the MSN framework permits indirect consideration of concurrent parameter influences. The MSN formulation relies on normalization within the dataset's minimum and maximum bounds; therefore, its application outside the calibrated parameter range should be performed with caution.

5. Results and model validation

The results and comparisons of the models are presented in Table 12, where the predicted values from the fitted curve and from the comprehensive models – comprising the constant coef-

Table 12. Data corresponding to mass parameter.

Tire		RR_0	RR_{Fitted}	$RR_{Constant}$	$RR_{Sigmoid}$	RR_{MSN}	$RMS_{Constant}$ [%]	$RMS_{Sigmoid}$ [%]	RMS_{MSN} [%]	Equalized mass
Test tires (sidewall)	225/55R19	9.45	9.460	8.63	9.820	9.699	7.5	5.5	4.1	12.64
	225/60R18	9.52	9.338	8.60	9.790	9.667				
	225/65R17	9.60	9.251	8.58	9.770	9.644				
	225/70R16	9.10	9.182	8.57	9.75	9.63				
	225/75R15	8.81	9.146	8.56	9.75	9.61				
Test tires (diameter)	205/60R13	8.9	9.809	9.49	9.340	9.37	3.6	3.8	3.7	8.715
	205/60R14	9.14	9.514	9.36	9.262	9.288				
	205/60R15	9.31	9.191	9.27	9.180	9.20				
	205/60R16	9.20	8.893	9.19	9.10	9.12				
	205/60R17	9.50	8.495	9.07	9.01	9.03				
Test tires (seated width)	205/55R16	9.22	9.236	9.28	9.123	9.166	5.4	5.7	6.0	8.35
	205/55R16	8.85	8.753	9.07	9.00	9.03				
	205/55R16	8.40	8.511	8.95	8.94	8.97				
	205/55R16	8.22	8.230	8.83	8.88	8.909				
	205/55R16	8.17	8.132	8.78	8.86	8.888				
Test tires (mass)	205/50R17	9.15	9.15	9.44	9.423	9.43	2.2	1.8	1.8	9.07
	205/50R17	9.43	9.393	9.44	9.482	9.48				9.34
	205/50R17	9.65	9.645	9.45	9.54	9.54				9.62
Out-of-test tires	225/65R17	9.6	N/A	8.59	9.895	9.747	7.0	3.7	2.8	13.05
	205/60R17	9.5		9.08	9.274	9.30				9.81
	205/60R15	9.31		9.27	9.19	9.21				8.715
	205/55R16	8.85		9.06	9.01	9.00				8.35
	235/50R19	10.13		8.69	9.98	9.91				12.500
	165/65R13	9.7		10.12	9.13	9.54				5.360
	215/55R18	8.84		8.756	9.38	9.379				11.135
	215/55R18	9.08		8.758	9.434	9.40				11.350
	215/55R18	9.21		8.759	9.58	9.48				11.530

ficients, sigmoid variable coefficients, and MSN variable coefficients for 27 tires (comprising the 21 test tires and 6 additional tires not used in model calibration) – are evaluated against the measurements obtained with the RR testing apparatus. It should be noted that, to verify the models, the second series of tires from the mass test, with a size of 215/55R18 (without accounting for mass changes), along with the 6 additional tires not used in model calibration, were used in addition to the test tires.

In addition, Fig. 7 and Fig. 8 show scatter plots comparing the RR values of the models and the experimental results for both the test tires and the additional tires not used in model calibration.

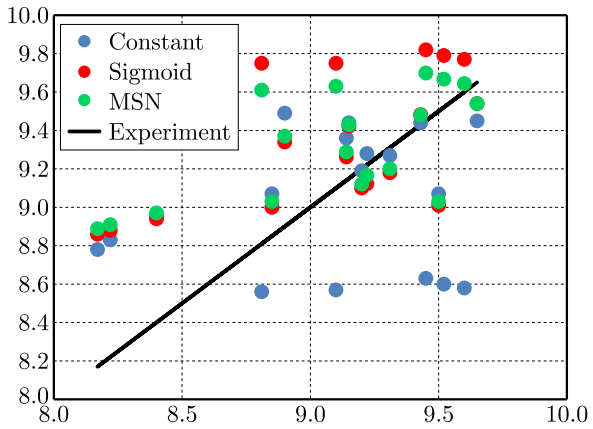

Fig. 7. Comparison of RR predictions using constant, sigmoid, and MSN weighting approaches. The MSN model shows improved agreement with experimental data across the investigated parameter range.

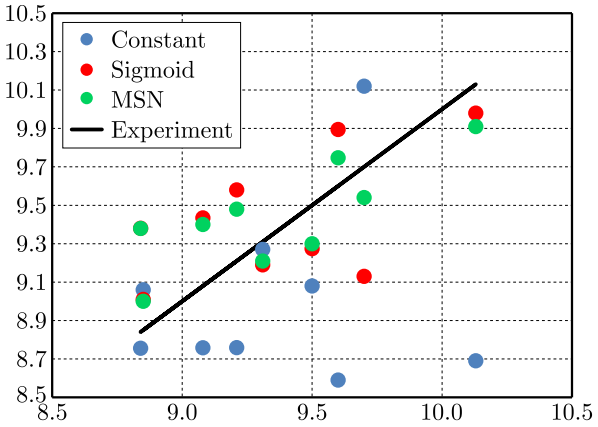

Fig. 8. Validation of the proposed model using independent tire data not included in the calibration set. The MSN approach demonstrates improved predictive performance compared to conventional methods within the studied domain.

Figure 7 compares the predictive performance of the constant, sigmoid, and MSN weighting approaches. The MSN model provides closer agreement with experimental data across the parameter range. This improvement can be attributed to the data-adaptive nature of the MSN weighting mechanism, which enables the model to capture variations in parameter influence better.

As shown in Fig. 8, the validation results using independent tire data demonstrate that the MSN model achieves the lowest prediction error among the evaluated approaches. This indicates that the proposed method has improved predictive capability beyond the calibration dataset. Nevertheless, it should be noted that the validation is limited to the investigated parameter range.

According to Table 12, the predictive accuracy of the MSN model is markedly higher for tires that were not used in model calibration than for the other two models. For these tires, the MSN model exhibits an error of 2.8 %, while the sigmoid model attains 3.7 % and the constant coefficient model 7 %. The MSN model's ability to predict tire RR, not used in the formulation of the comprehensive analytical model, demonstrates its potential for development and generalization, highlighting it as a key strength of the approach. The constant coefficient model, while offering a fast, straightforward methodology suitable for multiple variables with linear variation, exhibits the lowest accuracy among the models studied.

6. Discussion

The results of this study provide new insights into how tire mass and geometric parameters collectively influence RR. The developed analytical framework integrates individual empirical relations for tire mass, sidewall, diameter, and seated width into a unified formulation. Compared to previous approaches that primarily treated these parameters independently, the present model captures their combined influence within a consistent structure. However, the interactions are represented semi-empirically.

The experimental analysis revealed that increases in tire mass consistently lead to higher RR values, primarily due to greater internal energy dissipation and viscoelastic deformation during rotation. This observation is consistent with the thermomechanical understanding that heavier tires experience larger cyclic strain amplitudes, which increase hysteresis losses and heat generation in the tread and carcass layers. Within the investigated range, the approximately linear relationship between mass and RR suggests that the dominant energy-loss mechanisms scale proportionally with tire mass; however, extrapolation beyond this range should be approached with caution.

The effects of geometric parameters – sidewall, diameter, and seated width – were also systematically evaluated. Increasing the tire sidewall reduces flexibility and increases structural stiffness, thereby reducing RR. Similarly, larger tire diameters reduce RR by decreasing deformation per unit revolution. At the same time, increasing seated width lowers RR by enlarging the contact area, distributing the load more uniformly, and reducing localized deformation. These trends are generally consistent with previous studies (e.g., Walter (1983) and Ebbott *et al.* (1999)), while the present work extends them by incorporating tire mass into the same analytical framework.

The proposed MSN demonstrated the best overall agreement with experimental data, achieving an average prediction error below 3%. In contrast to constant and sigmoid weighting approaches, the MSN formulation dynamically adjusts weighting coefficients based on the parameter values and their normalized ranges. This feature enables the model to partially capture nonlinear interactions among variables, although it does not explicitly represent physical coupling mechanisms. As a result, the MSN framework offers improved predictive capability within the studied parameter space. Nevertheless, since the formulation relies on normalization within the dataset's minimum and maximum bounds, its application outside the calibrated range requires careful validation. Furthermore, extension of the model to different tire categories or operating conditions would require additional experimental data and recalibration of the weighting functions.

7. Conclusion

This research developed and validated a comprehensive analytical model capable of predicting tire RR while accounting for mass and geometric parameters. Experimental measurements were performed using an ISO 28580-based RR testing apparatus on 21 passenger tires, providing the foundation for analytical modeling. Curve-fitting methods were applied to derive

individual functional relationships between RR and each geometric parameter and tire mass; these relationships were subsequently integrated into a comprehensive analytical model. Three approaches were explored to determine the weighting coefficients that quantify each parameter's contribution within the model: constant coefficients, variable sigmoid-based coefficients, and a novel MSN. The MSN approach, introduced in this study, enables the derivation of dynamic weighting coefficients based on tire behavior within the considered dataset.

Model validation was performed by comparing the analytical predictions with experimental measurements for 27 tires (21 test tires and 6 additional tires not used in model calibration). The validation dataset includes tires with varying geometric and structural characteristics, providing an initial assessment of the model's predictive capability beyond the calibration set. The results indicate that the MSN model provides greater predictive accuracy than the other approaches. While the number of validation samples is limited, the results consistently show that the MSN model performs better than the alternative methods within the studied range. The MSN model achieves an RMS error of 2.8 %, whereas the sigmoid and constant coefficient models yield RMSE values of 3.7 % and 7 %, respectively.

The proposed approach provides a practical analytical framework for evaluating the influence of design parameters on RR. However, it should be noted that the model is semi-empirical in nature and is validated within the studied dataset and parameter ranges; therefore, its applicability beyond these conditions requires further investigation. In particular, the current formulation does not explicitly account for environmental and operating conditions such as temperature, inflation pressure, speed, and road surface, which may affect RR behavior.

The analytical framework presented here can serve as a basis for future research on multi-parameter tire optimization. Further studies may extend the MSN formulation by incorporating additional parameters and by validating the model using larger, more diverse datasets. In addition, coupling the proposed approach with finite element simulations or vehicle energy models could enhance its applicability for practical tire design and energy-efficiency assessments.

References

1. Ebbott, T.G., Hohman, R.L., Jeusette, J.-P., & Kerchman, V. (1999). Tire temperature and rolling resistance prediction with finite element analysis. *Tire Science and Technology*, *27*(1), 2–21. https://doi.org/10.2346/1.2135974

2. Ejsmont, J., Ronowski, G., Berge, T., Sommer, S., Owczarzak, W., & Szerszyńska, A. (2025). At what temperature should the tire rolling resistance be measured? *Proceedings of the Institution of Mechanical Engineers, Part D: Journal of Automobile Engineering*, *239*(12), 5961-5969. https://doi.org/10.1177/09544070241280316

3. Ejsmont, J., Ronowski, G., Ydrefors, L., Owczarzak, W., Sommer, S., & Świeczko-Żurek, B. (2024). Comparison of tire rolling resistance measuring methods for different surfaces. *International Journal of Automotive Technology*, *25*(4), 965–976. https://doi.org/10.1007/s12239-024-00092-w

4. Jittham, P., Sucharitpwatskul, S., Siriruk, S., & Meesaringkarn, S. (2022). Finite element analysis of elastomer: Case study – Rolling resistances of pneumatic and solid tyres. *IOP Conference Series: Materials Science and Engineering*, *1234*, Article 012002. https://iopscience.iop.org/article/10.1088/1757-899X/1234/1/012002

5. Liang, Ch., Li, H., Mousavi, H., Wang, G., & Yu, K. (2020). Evaluation and improvement of tire rolling resistance and grip performance based on test and simulation. *Advances in Mechanical Engineering*, *12*(12). https://doi.org/10.1177/1687814020981173

6. Luchini, J.R., Motil, M.M., & Mars, W.V. (2001). Tread depth effects on tire rolling resistance. *Tire Science and Technology*, *29*(3), 134–154. https://doi.org/10.2346/1.2135235

7. Ma, G., Xu, H., & Cui, W. (2007). Computation of rolling resistance caused by rubber hysteresis of truck radial tire. *Journal of Zhejiang University – SCIENCE A*, *8*, 778–785. https://doi.org/10.1631/jzus.2007.A0778

8. Mangal, Sh., Ghosh, P., Narasimha Rao, K.V., & Mukhopadhyay, R. (2021). Variable modulus approach to optimize tire rolling resistance. *Tire Science and Technology*, *49*(1), 39–54. https://doi.org/10.2346/tire.19.180200

9. Martini, M.E. (1983). Passenger tire rolling loss: A tread compounding approach and its trade-offs. In D.J. Schuring (Ed.), *Tire rolling resistance* (pp. 181–197). American Chemical Society. https://books.google.com/books/about/Tire_Rolling_Resistance_Rubber_Division.html?id=gSkBMgAACAAJ

10. Pillai, P.S., & Fielding-Russell, G.S. (1992). Tire rolling resistance from whole-tire hysteresis ratio. *Rubber Chemistry and Technology*, *65*(2), 444–452. https://doi.org/10.5254/1.3538623

11. Shida, Z., Koishi, M., Kogure, T., & Kabe, K. (1999). A rolling resistance simulation of tires using static finite element analysis. *Tire Science And Technology*, *27*(2), 84–105. https://doi.org/10.2346/1.2135980

12. Walter, J.D., & Conant, F.S. (1974). Energy losses in tires. *Tire Science and Technology*, *2*(4), 235–260. https://doi.org/10.2346/1.2167188

13. Walter, S.L. (1983). The effects of five basic design and construction parameters on radial tire rolling resistance and cornering force. *SAE Transactions*, *92*, 579–591. https://www.jstor.org/stable/44644395

14. Wang, G., Wu, X., Liang, Ch., & Yang, J. (2018). Design of low rolling resistance tire structure based on region energy loss. *Recent Patents on Mechanical Engineering*, *11*(2), 135–145. https://doi.org/10.2174/2212797611666180509161710

15. Xu, Y., Liu, Y., Gao, Y., Liu, L., & Zhang, L. (2025). Designing high-performance green tire treads by reinforcing the styrene-butadiene rubber/silica interface with chain difunctionalization. *Composites Part B: Engineering*, *290*, Article 111887. https://doi.org/10.1016/j.compositesb.2024.111887

16. Ydrefors, L., Hjort, M., Kharrazi, S., Jerrelind, J., & Stensson Trigell, A. (2021). Rolling resistance and its relation to operating conditions: A literature review. *Proceedings of the Institution of Mechanical Engineers, Part D: Journal of Automobile Engineering*, *235*(12), 2931–2948. https://doi.org/10.1177/09544070211011089

17. Ydrefors, L., Hjort, M., Kharrazi, S., Jerrelind, J., & Stensson Trigell, A. (2024). Measurement and evaluation of rolling resistance of car tyres at low operating temperatures. In W. Huang & M. Ahmadian (Eds.), *Advances in Dynamics of Vehicles on Roads and Tracks III* (pp. 845–856). Springer. https://link.springer.com/chapter/10.1007/978-3-031-66968-2_83

Manuscript received January 7, 2026; accepted for publication May 11, 2026;
published online June 17, 2026.